Advanced Hybrid MPPT Algorithms for High-Altitude Solar-Powered UAVs

Saranya Mukherjee
Institute of Radiophysics and Electronics
University of Calcutta
Kolkata, India
ORCID: 0009-0004-3408-0341

G A Reddy
ALD
CSIR- NAL
Bengaluru, India
email address or ORCID

Name Surname
dept. name of organization (of Aff.)
name of organization (of Aff.)
City, Country
email address or ORCID

***Abstract*—High-Altitude Long Endurance (HALE) Unmanned Aerial Vehicles (UAVs) rely on photovoltaic (PV) energy to sustain continuous operations, demanding lightweight and efficient power management. Extracting maximum solar power under rapidly changing irradiance and noisy sensor conditions remains challenging, as conventional Maximum Power Point Tracking (MPPT) algorithms either converge slowly, oscillate around the maximum power point, or impose high computational cost. Intelligent techniques such as fuzzy logic, artificial neural networks (ANN), and synergetic control improve performance, but none alone balances robustness, speed, and efficiency for aerospace applications. To address this gap, we propose a hybrid MPPT strategy integrating fuzzy logic with synergetic control, combining the adaptability of fuzzy inference with the fast, stable convergence of synergetic dynamics. Simulation results demonstrate that the hybrid controller achieves near-99% tracking efficiency with convergence in 0.03 s and minimal steady-state oscillation. Furthermore, the system maintains almost full performance until the signal-to-noise ratio (SNR) of input measurements falls to 18 dB, highlighting its robustness in noisy environments. These results confirm the suitability of the proposed hybrid algorithm for real-world HALE UAV missions where efficiency, weight, and reliability are critical.**

***Index Terms*—Maximum Power Point Tracking (MPPT), Fuzzy Logic, Synergetic Control, Hybrid Control, Photovoltaic Systems, High-Altitude Long Endurance (HALE) UAV.**

I. Introduction

Solar photovoltaic (PV) energy is essential for high-altitude long endurance (HALE) unmanned aerial vehicles (UAVs) to maintain continuous operations at stratospheric altitudes. Maximum power point tracking (MPPT) is a crucial subsystem for optimizing energy harvesting in situations with rapidly fluctuating temperature and irradiance. However, lightweight and effective MPPT algorithms are required due to the strict weight, power consumption, and onboard computational capacity restrictions of HALE UAVs [1]–[3].

Because of their simplicity, traditional MPPT algorithms like incremental conductance (IC) and perturb and observe (P&O) are still widely used [4]. However, these methods have serious shortcomings: While IC requires more computational work and still has trouble in dynamic conditions, P&O suffers from steady-state oscillations and is not very adaptable to sudden changes in irradiance [5].

To address these limitations, advanced MPPT techniques utilizing fuzzy logic, artificial neural networks, and swarm optimization have been investigated. Fuzzy logic controllers [6], [7] utilize rule-based systems to adaptively modify the output, ensuring robustness and modelling nonlinearity. However, they tend to fluctuate around the MPP, resulting in a loss of power and efficiency. Artificial neural networks (ANN) [8], [9] model nonlinear PV characteristics through feed-forward nets, achieving high accuracy but at the cost of significant computational cost at runtime. Swarm intelligence methods like particle swarm optimization (PSO) and ant colony optimization (ACO) [10]–[12] use bio-inspired global maximum tracking by iterative adjustment based on collective behavior. This offers both high accuracy and adaptability, but their iterative nature leads to very slow convergence times and thus lower efficiency. More intelligent algorithms like ACO inspired fuzzy logic systems [12] address the oscillation issue of fuzzy systems and sluggishness of ACO, but are computationally very intensive.

Alternatively, fractional order PID controllers [13], [14] use non-integer order integrals and differencials to model extreme non-linerarities and provide improved tracking but their range of linearity is limited. Synergetic control theory (SCT) [15]–[17] has recently emerged as a promising approach, delivering rapid convergence and low steady-state oscillations by enforcing system dynamics onto a convergent manifold. However, SCT may deviate from the exact MPP under certain conditions, especially when subject to buck converter configurations.

While each algorithm has their unique strengths, none alone fully satisfies the dual requirements of robustness and computational efficiency essential for HALE UAV missions. In our proposed algorithm, integrating fuzzy logic with synergetic control offers the potential to merge fuzzy adaptability with the dynamic stability of SCT, yielding a solution that is both efficient and lightweight for aerospace applications.

Table I summarizes the performance of representative MPPT methods in terms of convergence time, oscillation, and efficiency. Conventional and intelligent approaches address individual drawbacks but seldom achieve all three goals simultaneously. In contrast, the proposed hybrid Fuzzy-SCT method ensures fast tracking, low oscillations, and high efficiency with low computational cost.

This paper is structured as follows. Section II, details the solar cell model used for simulation. Sections III and IV

TABLE I: Comparative performance of MPPT algorithms from recent literature

Reference/Year	Method	MPPT Time	Steady-State Oscillation	Efficiency
[12]/2024	ACO based Fuzzy Logic	≈ 0.88 s	$\pm 1.0\%$	$\approx 98.6\%$
[9]/2023	Artificial neural network (ANN)	≈ 0.03 s	$\pm 0.7\%$	$> 90\%$
[11]/2022	Particle swarm optimization (PSO)	> 1.0 s	$\pm 1.6\%$	$\approx 97.0\%$
[18]/2024	ANN with incremental conductance(IC)	≈ 0.066	$\pm 0.4\%$	$> 90\%$
[15]/2025	Synergetic Control Theory (SCT)	$\approx 0.03s$	$\pm 0.1\%$	$\approx 98.1\%$
proposed work	Fuzzy + Synergetic Control	≈ 0.02 s	$\pm 0.087\%$	$\approx 98.94\%$

describe the individual fuzzy logic and synergetic control MPPT algorithms. Section V presents the proposed hybrid FLC+SCT MPPT strategy. Section VI discusses the simulation results, and Section VII concludes the paper.

II. Solar Cell Model

The photovoltaic source is represented using the single-diode model, which captures the nonlinear current-voltage characteristics of a solar cell. The output power P_{pv} is given by the equation:

$$P = n_p I_{pv} V - n_p I_0 \left(\exp\left(K_o \left(\frac{V}{n_s} + I_T R_{sT} \right) \right) - 1 \right) V - \left(\frac{V}{n_s} + I_T R_{sT} \right) \frac{V}{R_{shT}} \tag{1}$$

Where:

- P_{pv} is the output power
- V is the output voltage
- I_{pv} is the output current proportional to input irradiance
- I_T is the output current proportional to the temperature
- I_o is the reverse saturation current of the panel
- K_o is the diode ideality factor
- I_T is the thermal voltage
- R_{sT} is the series resistance
- R_{shT} is the shunt resistance
- n_s is the number of series
- n_p is the number of parallel cells

Equation (1) ensures that the I-V and P-V curves under varying irradiance and temperature conditions are realistically reproduced, allowing for meaningful comparison of tracking behaviors. A standard thin film solar cell designed for space applications, made by SHARP is chosen (Table II).

TABLE II: Solar Cell Parameters

Parameter	Value
I_{sc} (Short Circuit Current)	0.45 A
V_{oc} (Open Circuit Voltage)	3.05 V
I_{mpp} (MPP Current)	0.435 A
V_{pv} (MPP Voltage)	2.67 V
n_s (Number of Series Cells)	5
n_p (Number of Parallel Cells)	3

III. Fuzzy Logic-Based Algorithm

Fuzzy logic Controllers(FLC) [6] replace exact mathematical modeling with linguistic rule-based inference, using the incremental conductance(IC) structure is used as the core logic.

- MPP Error $E = \frac{dP}{dV} = I + V\frac{dI}{dV}$
- Change in error $\Delta E = E(k) - E(k-1)$

Thus, the input space of the FLC is:

$$\mathbf{x}(k) = \{E(k), \Delta E(k)\}. \tag{2}$$

The FLC generates a correction to the converter duty cycle:

$$\Delta D(k) \in \mathbb{R}, \tag{3}$$

which updates the duty ratio as:

$$D(k+1) = D(k) + \Delta D(k). \tag{4}$$

The control surface is shaped by triangular membership functions (Fig. 1), which define the degrees of linguistic variables. A triangular membership function for a linguistic value $A \in \mathcal{L}$ is defined as:

$$\mu_A(x) = \max\left(0, \min\left(\frac{x-a}{b-a}, \frac{c-x}{c-b}\right)\right), \quad x \in U \tag{5}$$

where (a, b, c) are the left, center, and right points of the triangle.

Here we have used 5-fold linguistic variables, namely:

- MNE: Medium Negative Error
- SNE: Small Negative Error
- ZE: Zero Error
- SPE: Small Positive Error
- MPE: Medium Positive Error

The rule base R consists of 25 rules of the form:

$$R_i: \text{ IF } E \text{ is } A_j \text{ AND } \Delta E \text{ is } B_k, \text{ THEN } \Delta D \text{ is } C_{jk}, \tag{6}$$

where $A_j, B_k, C_{jk} \in \mathcal{L}$. The complete mapping C_{jk} is given in Table III.

Using Mamdani's max-min composition for inference , the fuzzy inference process involves:

- Rule firing strength for rule R_i:

$$\alpha_i = \min\left(\mu_{A_j}(E(k)), \mu_{B_k}(\Delta E(k))\right). \tag{7}$$

- Implication: The output fuzzy set for rule R_i is

$$\mu'_{C_{jk}}(z) = \min(\alpha_i, \mu_{C_{jk}}(z)), \quad z \in U. \tag{8}$$

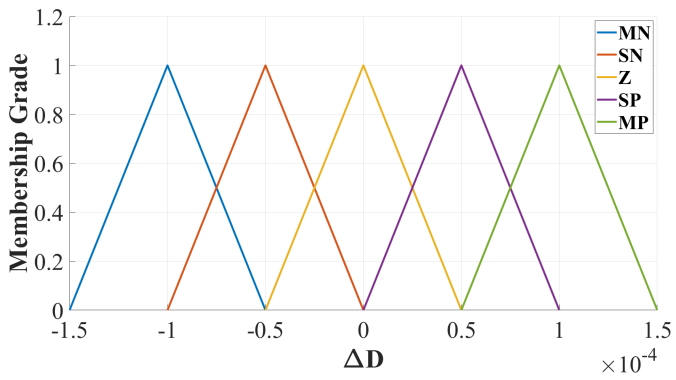

(a) Defuzzification function for FLC

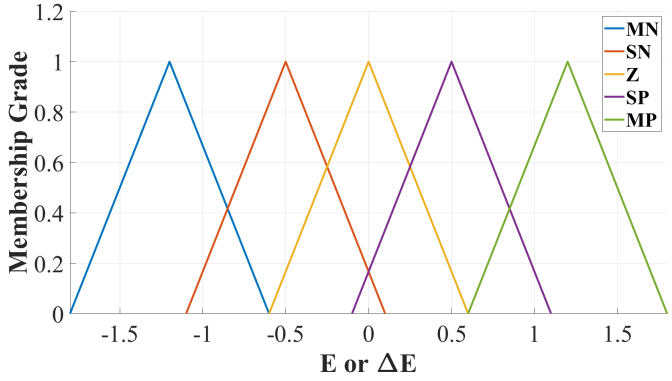

(b) Fuzzification function for FLC

Fig. 1: Membership functions for FLC

- Aggregation: The overall output fuzzy set is

$$\mu_{\Delta D}(z) = \max_i \mu'_{C_{jk}}(z). \tag{9}$$

Similarly, the crisp output is obtained using the centroid method:

$$\Delta D^*(k) = \frac{\int_U z\,\mu_{\Delta D}(z)\,dz}{\int_U \mu_{\Delta D}(z)\,dz}. \tag{10}$$

TABLE III: Fuzzy Rule Base for MPPT Controller

E\dE	**MNE**	**SNE**	**ZE**	**SPE**	**MPE**
MNE	MP	MP	SP	SP	Z
SNE	MP	SP	SP	Z	SN
ZE	MN	SN	Z	SN	MN
SPE	SN	Z	SP	SP	MP
MPE	Z	SP	SP	MP	MP

IV. Synergetic Control Theory (SCT) for Buck Converters

Synergetic control is a nonlinear control methodology [15] based on the theory of dynamical system decomposition and manifold enforcement. In MPPT applications, it allows for the creation of a global, converging control law without requiring full dynamic modeling.

To derive the required control law, first define the state space equations for a buck converter (as shown in Fig 2):

$$\frac{dI_L}{dt} = \frac{1}{L}(d.V_{in} - D_{dc}) \tag{11}$$

$$\frac{dV_{dc}}{dt} = \frac{1}{C}(I_L - \frac{V_{dc}}{R}) \tag{12}$$

- V_{dc} is the output voltage
- I_L is the inductor current (approximated as I_{pv})
- V_{in} is the input voltage (approximated as V_{pv})
- d is the duty cycle
- L-C are the inductor and capacitor values in the buck converter

Then define a macro-variable:

$$\psi = \frac{P_{pv}}{I_{pv}} \tag{13}$$

The control law is designed [15] to ensure that ψ converges to the MPP value, which is defined as:

$$T\dot{\psi} + \theta(\psi) = 0 \tag{14}$$

Where T is a designer chosen parameter that determines the rate of convergence to the invariant manifold $\psi(x,t) = 0$ specified by the macro-variable ψ. $\theta(\psi)$ is defined as a smooth differentiable function of that has to be selected, such that

- invertible and differentiable
- $\theta(0) = 0$
- $\theta(\psi)\psi > 0\ \forall\psi \neq 0$

With these constraints, the $\theta(\psi)$ function can be chosen as:

$$\theta(\psi) = \psi(x,t) \tag{15}$$

Using these equations a custom control law has been derived for the buck converter setup as follows:

$$d = \frac{1}{V_{pv}}\left(V_{dc} - \frac{L}{T}\cdot\frac{\left(V_{pv} + I_{pv}\frac{dV_{pv}}{dI_{pv}}\right)}{2\frac{dV_{pv}}{dI_{pv}} + I_{pv}\frac{d^2V_{pv}}{dI_{pv}^2}}\right) \tag{16}$$

After optimization, the control law converges to the MPP with a guaranteed stability margin (T = 0.0005).

V. Hybrid FLC-SCT based algorithm

To exploit the strengths of both fuzzy logic control (FLC) and synergetic control theory (SCT), a hybrid MPPT controller is formulated. The fuzzy controller provides smooth convergence in the vicinity of the maximum power point (MPP), while the synergetic controller ensures fast dynamics when the operating point is far from the MPP.

Let the error signal $E(k)$ be defined as in Section III. Two thresholds e_1 and e_2 are introduced, with $e_1 < e_2$, to form a

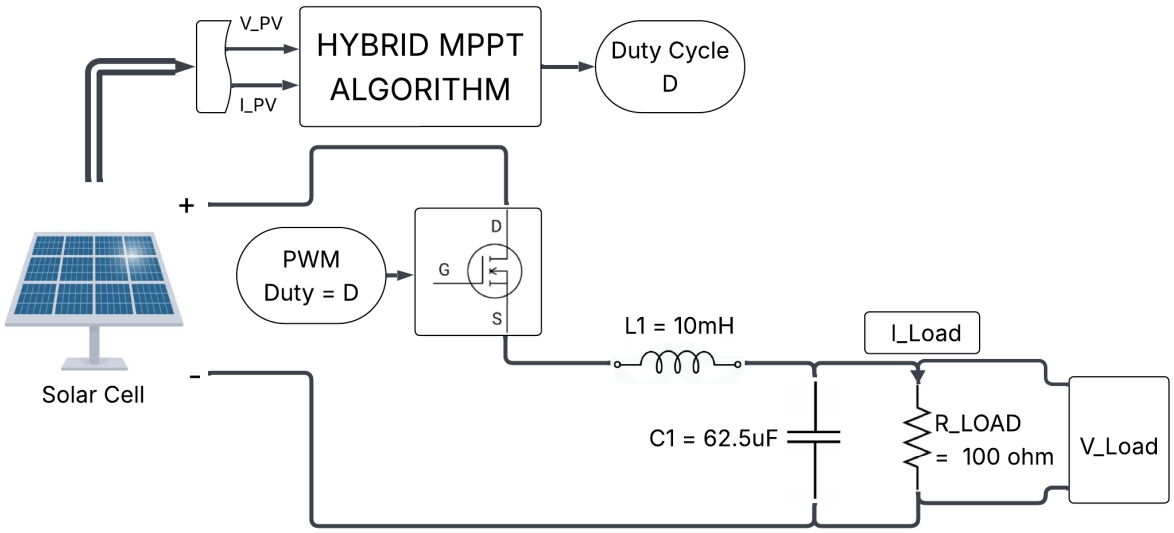

Fig. 2: Buck converter-based MPPT system architecture

band around the MPP:

$$u(k) = \begin{cases} u_{\text{FLC}}(k), & e_1 \le |E(k)| \le e_2, \\ u_{\text{SCT}}(k), & |E(k)| < e_1 \ \text{ or } \ |E(k)| > e_2, \end{cases} \tag{17}$$

where $u(k)$ is the control value applied to the duty ratio. Here, $u_{\text{FLC}}(k)$ is obtained from the Mamdani fuzzy inference system as detailed in Section III, and $u_{\text{SCT}}(k)$ is obtained from the synergetic control law derived in Section IV.

The converter duty ratio is updated according to the selected control strategy:

$$D(k+1) = \begin{cases} D(k) + u_{\text{FLC}}(k), & \text{if FLC is used} \\ u_{\text{SCT}}(k), & \text{if SCT is used} \end{cases} \tag{18}$$

To mitigate high-frequency switching noise and jitter at steady state, a low-pass FIR filter is applied to the duty cycle. Let $D_f[k]$ denote the filtered duty cycle sequence and $D[k]$ denote the updated duty cycle sequence. A length-M FIR low-pass filter with Dolph-Chebyshev window is defined as

$$h[n] \;=\; h_d[n]\, w[n], \qquad n = 0, \ldots, M-1,$$

where the ideal low-pass response is

$$h_d[n] \;=\; \begin{cases} \dfrac{\omega_c}{\pi}, & n = m_0, \\ \dfrac{\sin\big(\omega_c (n - m_0)\big)}{\pi (n - m_0)}, & n \neq m_0, \end{cases}$$

with $m_0 = (M-1)/2$. The Dolph-Chebyshev window is

$$w[n] \;=\; \frac{T_{M-1}\Big(\beta \cos \frac{\pi (n - m_0)}{M-1}\Big)}{T_{M-1}(\beta)},$$

where $T_{M-1}(\cdot)$ is the Chebyshev polynomial of order $M-1$. The parameters are

$$\omega_c = 2\pi \frac{f_c}{f_s}, \qquad \beta = \cosh\Big(\tfrac{1}{M-1} \operatorname{arccosh}(10^{A/20})\Big),$$

with f_c the cutoff frequency, f_s the sampling frequency, and A the sidelobe attenuation (dB). Finally, the filtered duty cycle is

$$D_f[k] \;=\; \sum_{m=0}^{M-1} h[m]\; D[k-m].$$

f_c and A are chosen to balance noise rejection with response time to give optimal performance at 2kHz and 50dB respectively.

Algorithm 1 Hybrid FLC-SCT MPPT algorithm with dual thresholds

while true **do**
  Measure V_{PV}, I_{PV} and compute error $E(k)$
  if $e_1 \le |E(k)| \le e_2$ **then**
    Compute control increment $u(k) \leftarrow u_{\text{FLC}}(k)$ {Fuzzy inference (see Section III)}
    Update duty cycle: $D(k+1) \leftarrow D(k) + u(k)$
  else
    Compute control increment $u(k) \leftarrow u_{\text{SCT}}(k)$ {Synergetic control (see Section IV)}
    Update duty cycle: $D(k+1) \leftarrow u(k)$
  end if
  Apply FIR low-pass filter to $D(k+1)$ to obtain $D_f(k+1)$
  Set duty cycle for next iteration: $D(k+1) \leftarrow D_f(k+1)$
end while

VI. Results and Discussion

In order to evaluate the quality and practicality of each MPPT method, the subsequent metrics are recorded:

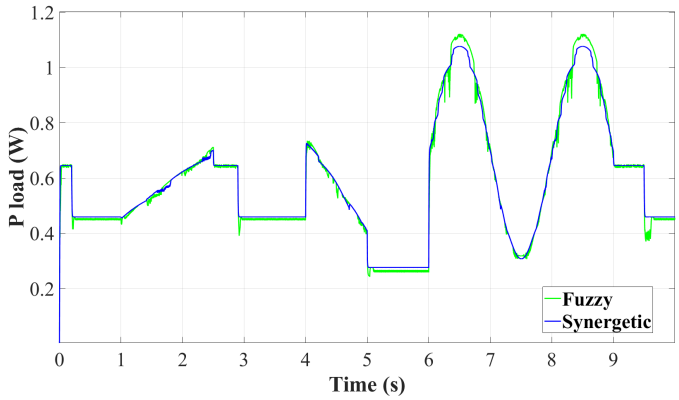

(a) Irradiance tracking of FLC and SCT algorithms

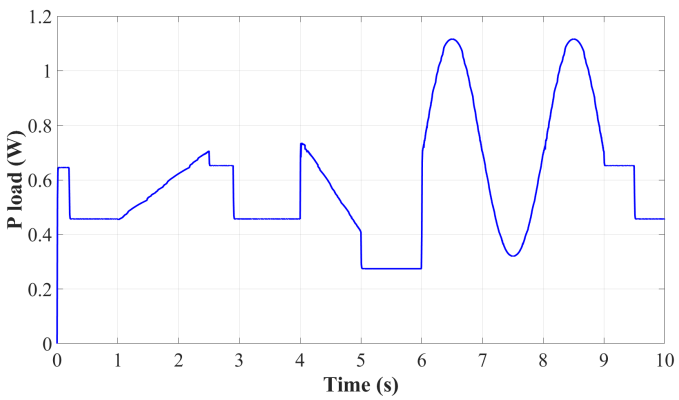

(b) Irradiance tracking of FLC + SCT hybrid

Fig. 3: MPPT algorithm irradiance tracking curves

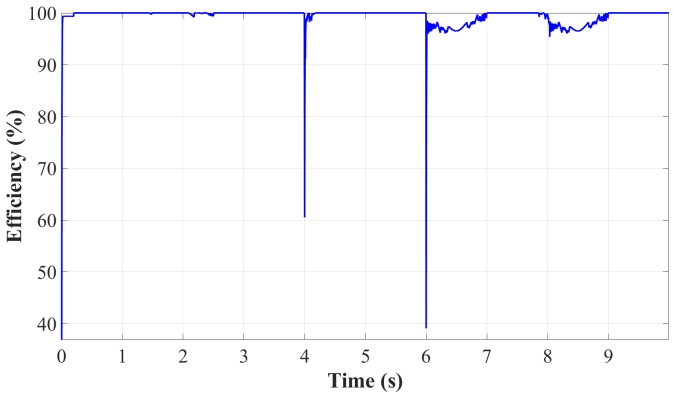

(a) FLC + SCT efficiency curve with no added noise

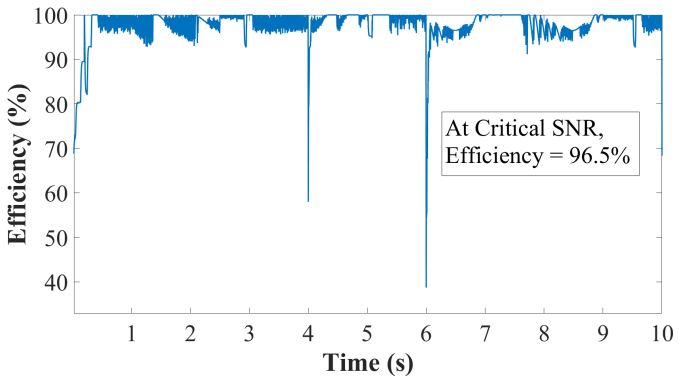

(b) FLC + SCT efficiency curve at critical SNR

Fig. 4: FLC + SCT hybrid efficiency curves

TABLE IV: Comparison of hybrid MPPT algorithms

Algorithm	Efficiency	Convergence Time (s)	Steady-State Oscillations
FLC + SCT	98.94%	0.021s	0.087%
ANN + FOPID [19]	98.1%	0.049s	0.386%
ANN + SMC [20]	96.2%	0.22s	–
FOPID [13]	97.96%	0.03s	0.7%

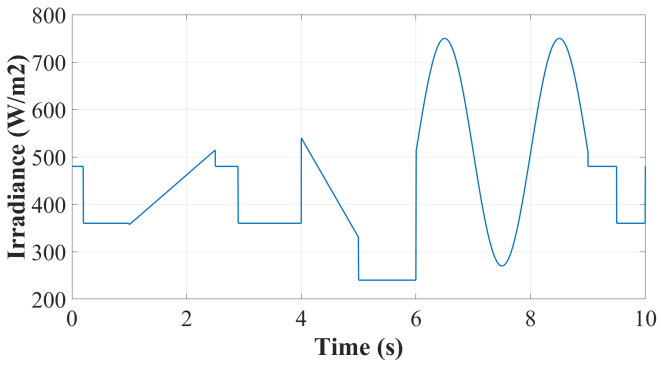

Fig. 5: Irradiance curve for efficiency comparison

- **Efficiency:**
  Ratio of extracted power to the theoretical maximum available. Fig 5 shows the irradiance profile used for efficiency comparisons.
- **Convergence Time:**
  Time taken to reach the maximum power point under changing conditions. It is measured as the time taken by the algorithm to reach 95% of the MPP from 5%.
- **Steady-State Oscillation:**
  Steady-state fluctuations around the MPP expressed as a percentage of the MPP. More the steady-state oscillations, more the power loss.
- **Robustness:**
  The minimum SNR of the input V and I signals that the algorithm can process without losing more than 2% of

TABLE V: Noise tolerance results for MPPT algorithms

Algorithm	SNR Voltage (dB)	SNR Current (dB)
FLC + SCT	33 dB	18 dB
ANN + SCT	34 dB	23dB
PIλ + SCT	40 dB	31dB
SCT	36 dB	23 dB
FLC	42 dB	26dB

TABLE VI: Results of hybrid FLC-SCT algorithm

System Parameter	Value
Efficiency	98.94%
Convergence time (s)	0.021 s
Steady State Error (%)	$\pm$0.087%
Noise Tolerance	upto 18dB SNR

its noise-free baseline characterizes its behavior under noise or disturbances. In real-world scenarios, where measurement noise is unavoidable, this metric shows how well the algorithm maintains dependable MPPT. (The better the noise tolerance, the lower the SNR value.)

Fig 3 illustrates the tracking accuracy of the FLC+SCT hybrid algorithm as compared to its individual components. Fig 4 shows the efficiency curves of the FLC+SCT hybrid algorithm under no noise and critical noise conditions, demonstrating its robustness. Table IV and table V compares the FLC+SCT to other state of the art hybrid and individual algorithms, showing its superior performance across all metrics. Table VI summarizes the key performance metrics of the proposed FLC+SCT hybrid algorithm.

VII. Conclusion

The FLC + SCT hybrid stands out as the most effective MPPT strategy for HALE UAVs, combining the adaptability of fuzzy logic with the rapid and stable convergence of synergetic control. The primary benifits are:

- Swift convergence to the maximum power point, even amidst rapidly fluctuating irradiance.
- Exceptional tracking accuracy, maintaining a steady-state error consistently under 0.1%.
- Achieved nearly 99% efficiency across various operating scenarios.
- Exhibits robust noise resilience, ensuring dependable performance even at 18 dB SNR.

Considering practical aerospace constraints like weight, power, and robustness, the FLC + SCT hybrid emerges as a highly deployable and comprehensive MPPT solution for solar-powered HALE UAV systems.

VIII. Future Work

Future work will focus on implementing the proposed FLC + SCT hybrid MPPT on embedded hardware to evaluate real-time performance. Adaptive tuning methods, such as machine learning-based optimization of fuzzy and synergetic parameters, may further enhance tracking under dynamic conditions. Additional efforts will explore integration with UAV flight control, robustness under extreme noise/temperature, and long-duration simulations or flight trials to assess real-world energy gains and mission endurance.

References

[1] S. Alnaser and A. Omer, "Photovoltaic energy harvesting for aerospace applications: Challenges and opportunities," *Energy Reports*, vol. 7, pp. 1174–1188, 2021.

[2] H. Wang, Y. Liu, and L. Zhao, "High-efficiency mppt strategies for solar-powered uavs under dynamic irradiance," *Journal of Power Electronics*, vol. 22, no. 5, pp. 1001–1013, 2022.

[3] J. Liang, K. Xu, and Y. Zhang, "Advances in high-altitude long endurance (hale) uavs: Energy management and photovoltaic system integration," *IEEE Access*, vol. 11, pp. 15 245–15 260, 2023.

[4] J. Ahmed and Z. Salam, "A comprehensive review of maximum power point tracking algorithms for photovoltaic systems," *Renewable and Sustainable Energy Reviews*, vol. 74, pp. 1142–1158, 2020.

[5] C. Zhang, J. Wang, and H. Liu, "Improved incremental conductance mppt algorithm for solar uavs under dynamic conditions," *International Journal of Photoenergy*, vol. 2021, pp. 1–12, 2021.

[6] M. Y. Allani, D. Mezghani, F. Tadeo, and A. Mami, "Fpga implementation of a robust mppt of a photovoltaic system using a fuzzy logic controller based on incremental and conductance algorithm," *Engineering, Technology & Applied Science Research*, vol. 9, no. 4, pp. 4322–4328, 2019.

[7] Y. Zhou, H. Chen, and P. Xu, "Enhanced fuzzy logic mppt algorithm for solar pv systems in dynamic weather," *Energy Conversion and Management*, vol. 251, p. 114965, 2022.

[8] A. Demirci, I. Dagal, S. Mirza Tercan, H. Gundogdu, M. Terkes, and U. Cali, "Enhanced ann-based mppt for photovoltaic systems: Integrating metaheuristic and analytical algorithms for optimal performance under partial shading," *IEEE Access*, vol. 13, pp. 92 783–92 799, 2025.

[9] P. Chauhan, R. Singh, and S. Yadav, "Artificial intelligence-based mppt algorithms for solar energy harvesting: A review and new perspectives," *Applied Energy*, vol. 336, p. 120857, 2023.

[10] I. Saady, B. Majout, B. Bossoufi, M. Karim, I. Elkafazi, S. Merzouk, M. M. Almalki, T. A. Alghamdi, P. Skruch, A. Zhilenkov *et al.*, "Improving photovoltaic water pumping system performance with pso-based mppt and pso-based direct torque control using real-time simulation," *Scientific Reports*, vol. 15, no. 1, p. 16127, 2025.

[11] R. Sharma, P. Gupta, and V. Singh, "Hybrid intelligent mppt algorithms for photovoltaic systems: A review and future prospects," *Journal of Cleaner Production*, vol. 340, p. 130744, 2022.

[12] K. Xia, Y. Li, and B. Zhu, "Improved photovoltaic mppt algorithm based on ant colony optimization and fuzzy logic under conditions of partial shading," *IEEE Access*, vol. 12, pp. 44 817–44 825, 2024.

[13] O. Saleem, S. Ali, and J. Iqbal, "Robust mppt control of stand-alone photovoltaic systems via adaptive self-adjusting fractional order pid controller," *Energies*, vol. 16, no. 13, p. 5039, 2023.

[14] A. Rawat, S. Jha, B. Kumar, and V. Mohan, "Nonlinear fractional order pid controller for tracking maximum power in photo-voltaic system," *Journal of Intelligent & Fuzzy Systems*, vol. 38, no. 5, pp. 6703–6713, 2020.

[15] A.-B. A. Al-Hussein, F. R. Tahir, and V.-T. Pham, "Fpga implementation of synergetic controller-based mppt algorithm for a standalone pv system," *Computation*, vol. 13, no. 3, p. 64, 2025.

[16] R. Ayat, A. Bouafia, and J.-P. Gaubert, "Experimental validation of synergetic approach based mppt controller for an autonomous pv system," *IET Renewable Power Generation*, vol. 15, no. 7, pp. 1515–1527, 2021.

[17] K. Bharath, P. Venkatesh, and S. Kumar, "Synergetic control-based mppt for photovoltaic systems under dynamic irradiance," *ISA Transactions*, vol. 112, pp. 102–114, 2021.

[18] B. M. Bellah, B. Tahar, and B. Adel, "Adaptive hybrid mppt using artificial intelligence for an autonomous pv system," *International Journal of Smart Grid-ijSmartGrid*, vol. 8, no. 1, pp. 27–34, 2024.

[19] R. Bisht, A. Sikander, A. Sharma, K. Abidi, M. R. Saifuddin, and S. S. Lee, "A new hybrid framework for the mppt of solar pv systems under partial shaded scenarios," *Sustainability*, vol. 17, no. 12, p. 5285, 2025.

[20] L. Chen and X. Wang, "An enhanced mppt method based on ann-assisted sequential monte carlo and quickest change detection," *arXiv preprint arXiv:1805.04922*, 2018.